J. Fluid Mech. (1972), *vol.* 54, *part* 1, *pp.* 63–80
Printed in Great Britain

Wave propagation across the continental shelf

By JOHN W. MILES
Institute of Geophysics and Planetary Physics, University of California, La Jolla

(Received 17 December 1971)

Wave propagation across the continental shelf is studied by analogy with transmission-line theory. Fourier transformation along the contours of constant depth, which are assumed parallel to a straight coastline, yields a Sturm–Liouville equation for a prescribed depth profile $h(x)$. The modal spectrum of the profile, which comprises a finite, discrete spectrum of trapped modes and a continuous spectrum of radiated modes, is established. The Green's function for a point source on the coastline is constructed by Fourier superposition over this spectrum. Detailed results are calculated for a two-step model (level shelf separated from level abyss by vertical cliff) and for a gradually sloping shelf that merges smoothly into a level abyss. The radiation impedance of a harbour is calculated, and the effects of the continental shelf on the resonant response of the harbour to a tsunami are discussed.

1. Introduction

The following treatment of long waves on a continental shelf is directed primarily towards the calculation of the Green's function for a point source on the coastal boundary with specific application to the resonant response of a harbour to tsunami excitation. It is possible, however, that the preliminary results developed in §§3 and 4 may be of somewhat wider interest.

By *long waves*, we imply disturbances that are sufficiently long to justify shallow-water theory, but not so long as to render Coriolis effects significant. Starting from the hypotheses implicit in this definition and neglecting viscosity, we develop in §2 the equations governing wave propagation in a half-space $x > 0$ with depth contours $h = h(x)$ parallel to the boundary $x = 0$. In §3, after Fourier transformation with respect to y (the co-ordinate measured along contours of constant depth), we consider one-dimensional propagation over the profile $h = h(x)$ and develop an analogy with propagation along a transmission line with spatially varying properties. The (complex amplitudes of the) free-surface displacement and a normalized measure of the mass transport at a given point, say x_m, form a two-element column matrix, say $\boldsymbol{\varphi}_m$, such that $\boldsymbol{\varphi}_n = \mathbf{T}_m^n \boldsymbol{\varphi}_m$, where $\mathbf{T}_n^m$ is a 2×2 transfer matrix for the interval (x_m, x_n). The requirement that $\boldsymbol{\varphi}(x)$ be continuous across discontinuities in $h(x)$ implies that the transfer matrices for a set of sub-intervals may be cascaded over any interval in which $h(x)$ is piecewise continuous.

In §4, we consider the free modes of a given profile with the boundary conditions of no mass transport across $x = 0$ and either a radiation or a finiteness condition

at $x = \infty$. The total spectrum of these free modes comprises a discrete spectrum of trapped modes and a continuous spectrum of radiated (or standing-wave) modes. The discrete spectrum is finite for a shelf of finite length and contains at least one mode except in the limiting case of constant depth.

In §5, we construct the Green's function, say G, for a point source on the boundary $x = 0$ by Fourier superposition over the complete spectrum of modes for a given profile. We then establish a local approximation to G that differs from the corresponding Green's function of potential theory by a complex constant, the value of which determines the radiation impedance of a finite source distribution over a coastal interval (such as a harbour mouth) that is small compared with the wavelength.

In §6, we consider a two-step model, which comprises a shelf of constant depth that drops discontinuously into an abyss of constant depth. In §7, we develop the WKB approximation for a shelf of gradually varying depth that merges smoothly into an abyss of constant depth at a finite distance from the coast and apply the results to a parabolic shelf (the solution for a parabolic shelf may be expressed in terms of Bessel functions without invoking the WKB approximation, but the results are rather cumbersome).

In §8, we apply the development of §§5–8 to the calculation of the radiation impedance for a harbour mouth and consider the effects of variable depth, *vis-à-vis* those for an ocean of constant depth (Miles 1971), on Helmholtz resonance under tsunami excitation. The principal differences are an increase of each of the resonant frequency, the inverse damping factor Q, and power-spectrum amplification factor $\mathscr{P}$. The reader who is interested primarily in the qualitative effects of a continental shelf on harbour resonance could turn directly to §8.

2. Formulation

Let x and y be Cartesian co-ordinates in the free surface, with x measured seaward from the coastline ($x = 0$), t the time, σ the angular frequency, $h(x)$ the local depth, $\hat{\zeta}$ the free-surface displacement, $\hat{\mathbf{u}}$ the horizontal particle velocity, and ζ and $\mathbf{u}$ the corresponding complex amplitudes, such that

$$\{\hat{\zeta}(x,y,t), \hat{\mathbf{u}}(x,y,t)\} = \mathscr{R}[\{\zeta(x,y), \mathbf{u}(x,y)\}\, e^{i\sigma t}], \tag{2.1}$$

where $\mathscr{R}$ implies *the real part of*. The linearized, shallow-water equations for ζ and $\mathbf{u}$ are (Lamb 1932, §193)

$$i\sigma\mathbf{u} = -g\nabla\zeta \tag{2.2a}$$

and

$$h^{-1}(h\zeta_x)_x + \zeta_{yy} + k^2\zeta = 0, \tag{2.2b}$$

where

$$k = k(x) = \sigma\{gh(x)\}^{-\frac{1}{2}} \tag{2.3}$$

is the local wavenumber.

Separating variables according to

$$\zeta(x,y) = \phi(x)\, e^{-i\beta y}, \tag{2.4}$$

we obtain

$$(h\phi')' + \alpha^2 h\phi = 0, \tag{2.5}$$

where

$$\alpha^2 = \alpha^2(x,\beta) = k^2(x) - \beta^2, \tag{2.6}$$

and the prime implies differentiation with respect to x. We also define

$$\psi(x) = h(x)\,\phi'(x) \tag{2.7}$$

as a measure of the mass transport normal to the coastline and

$$\chi(x) = -\psi(x)/\phi(x) = -h(x)\,\phi'(x)/\phi(x) \tag{2.8}$$

as the corresponding *impedance function*; χ satisfies the Riccati equation

$$h\chi' = \chi^2 + \kappa^2, \tag{2.9}$$

where
$$\kappa = \kappa(x) = \alpha(x,\beta)\,h(x) = \{(\sigma^2/g) - \beta^2 h(x)\}^{\frac{1}{2}}. \tag{2.10}$$

We assume that $h(x)$ is piecewise continuous, by virtue of which each of ϕ, ψ, and χ is a continuous function of x.

As posed, (2.4) represents a disturbance travelling in the positive-y direction (south on the Pacific coast for right-handed co-ordinates) if β is positive and real; changing the sign of β yields a wave travelling in the negative-y direction. A general solution can be constructed by Fourier-integral superposition, in which case β may be regarded as complex (see §5).

3. Impedance transformation

Describing the wave state at $x = x_m$ by the two-element column matrix

$$\{\phi(x_m), \psi(x_m)\} \equiv \{\phi_m, \psi_m\}, \tag{3.1}$$

we may express the solution in $(0, l)$ as a linear combination of $\phi^{0c}(x)$ and $\phi^{0s}(x)$, the cosine-line and sine-like solutions of (2.5) that satisfy the initial conditions

$$\phi_0^{0c} = 1, \quad \psi_0^{0c} = 0, \quad \phi_0^{0s} = 0, \quad \psi_0^{0s} = 1. \tag{3.2a,b,c,d}$$

We may then connect the wave states at $x = 0$ and $x = l$ by the linear transformation

$$\{\phi_l, \psi_l\} = \mathbf{T}_l^0\{\phi_0, \psi_0\}, \tag{3.3a}$$

where
$$\mathbf{T}_l^0 = \begin{bmatrix} \phi_l^{0c} & \phi_l^{0s} \\ \psi_l^{0c} & \psi_l^{0s} \end{bmatrix} \tag{3.3b}$$

is the *transfer matrix* for $(0, l)$, and the subscript l implies $x = l$. Invoking the Wronskian relation between $\phi^{0c}(x)$ and $\phi^{0s}(x)$, we obtain

$$|\mathbf{T}_l^0| = \phi_l^{0c}\psi_l^{0s} - \phi_l^{0s}\psi_l^{0c} = 1. \tag{3.4}$$

Invoking the requirement that $\mathbf{T}_0^l$ be the inverse of $\mathbf{T}_l^0$, together with (3.4), we obtain the reciprocity relations

$$\psi_0^{ls} = \phi_l^{0c}, \quad \phi_0^{ls} = -\phi_l^{0s}, \quad \psi_0^{lc} = -\psi_l^{0c}. \tag{3.5a,b,c}$$

Calculating ψ_l/ϕ_l from (3.3) and invoking (2.8) and (3.5), we obtain the impedance transformations

$$\chi_l = (-\psi_l^{0c} + \chi_0\psi_l^{0s})/(\phi_l^{0c} - \chi_0\phi_l^{0s}) \tag{3.6a}$$

$$= (\psi_0^{lc} + \chi_0\phi_0^{lc})/(\psi_0^{ls} + \chi_0\phi_0^{ls}). \tag{3.6b}$$

It follows from (2.5) and (3.2) that each of the elements of $\mathbf{T}_0^l$ is real for real values of β^2 and is an entire function of β (by virtue of the fact that α^2 is an entire function of β); accordingly, the only singularities of $\chi_l(\beta)$ are either the branch points, if any, of $\chi_0(\beta)$ or poles.

It may be expedient, in considering a given depth profile, to consider subintervals within which $h(x)$ may be approximated by a form that permits either an analytical or a numerical solution of (2.5). Invoking the requirement that ϕ and ψ be continuous across finite discontinuities of h, we may then cascade the transfer matrices according to

$$\mathbf{T}_n^0 = \mathbf{T}_n^{n-1}\mathbf{T}_{n-1}^{n-2}\ldots\mathbf{T}_1^0 \tag{3.7}$$

over any interval (x_0, x_n) in which $h(x)$ is piecewise continuous (cf. Munk, Snodgrass & Gilbert 1964). Similarly, the transformations (3.6a, b) may be cascaded to obtain a bilinear transformation between χ_0 and χ_n, although it may be simpler to proceed through (3.7).

4. Free modes

Free modes are those solutions of (2.5) that satisfy

$$\psi(0) = 0 \quad \text{and} \quad |\phi(x)| < \infty \quad (x \uparrow \infty). \tag{4.1a,b}$$

We consider these solutions on the assumption that $h_0 < h(x) < h_\infty$ in $(0, l)$, the *shelf*, and $h(x) = h_\infty$ in $x > l$, the *abyss*. The boundary condition (4.1a) implies that $\phi(x)$ must be proportional to $\phi^{0c}(x)$ in $(0, l)$, where $\phi^{0c}(x)$ is determined by (2.5) and (3.2a, b). The finiteness condition (4.1b), together with the assumption of constant depth, implies that $\phi(x)$ must be either exponentially decaying or trigonometric in (l, ∞).

The exponentially decaying solutions are known as *trapped modes* and have a finite, discrete spectrum, say

$$k_0^2 > \beta_1^2 > \beta_2^2 > \ldots \beta_n^2 > k_\infty^2, \tag{4.2}$$

where, by assumption, $k_\infty < k(x) < k_0$ in $(0, l)$. Designating these modes by $\phi(x, \beta_m)$ and choosing the normalization $\phi(0, \beta_m) = 1$, we obtain

$$\phi(x, \beta) = \begin{cases} \phi^{0c}(x) & (0 \leqslant x \leqslant l), \quad (4.3a) \\ \phi_l^{0c} e^{-\mu(x-l)} & (x \geqslant l), \quad (4.3b) \end{cases}$$

where

$$\mu = (\beta^2 - k_\infty^2)^{\frac{1}{2}} \equiv i\alpha_\infty, \tag{4.4}$$

and the β_m are determined by the impedance-matching condition

$$\chi_l^{0c} \equiv \psi_l^{0c}/\phi_l^{0c} = \mu h_\infty \equiv \chi_\infty \quad (\beta = \pm\beta_m). \tag{4.5}$$

We designate χ_l^{0c} as the *modal impedance* of the shelf.

By invoking standard arguments from Sturmian theory (Ince 1944, §10.32), we find that (4.5) has at least one root in (k_∞, k_0) and that a necessary condition for the existence of more than one root ($n > 1$) is

$$(k_0^2 - k_\infty^2)^{\frac{1}{2}} \equiv \alpha_* > \pi/l; \tag{4.6}$$

conversely, $\alpha_* < \pi/l$ implies $n = 1$. The ratio χ_l^{0c}/χ_∞ is small (of the order of h_s/h_∞, where h_s is the mean shelf depth) except in the neighbourhood of $\beta = \pm\beta_m$. It follows that β_n, the dominant eigenvalue, is close to k_∞, whilst the remaining eigenvalues are close to the poles, if any, of $\chi_l^{0c}(\beta)$; the latter modes resemble those of an open organ pipe. These facts are illustrated in figure 2 for the two-step model of §6. The mass transport for the mth mode, $\psi(x, \beta_m)$, has $m-1$ nodes in $(0, l)$.

The remaining free modes have a continuous spectrum in $0 \leqslant \beta^2 < k_\infty^2$ and are given by

$$\phi(x) = \begin{cases} \phi^{0c}(x) & (0 \leqslant x \leqslant l), \quad (4.7a) \\ \phi_l^{0c} \sec\epsilon \cos\{\alpha_\infty(x-l)+\epsilon\} & (x \geqslant l), \quad (4.7b) \end{cases}$$

where the phase parameter ϵ is determined by the impedance-matching condition

$$\chi_l^{0c} = \kappa_\infty \tan\epsilon. \tag{4.8}$$

We may regard the right-hand side of (4.7*b*) as the superposition of an incident wave and its reflexion at the virtual boundary $x = l-(\epsilon/\alpha_\infty)$. The corresponding reflexion coefficient is

$$R = \exp(-2i\epsilon), \tag{4.9}$$

whilst the amplification factor of the shelf (referred to the peak value of the disturbance in $x > l$) is

$$A(\beta) = \cos\epsilon/\phi_l^{0c} = \kappa_\infty\{(\kappa_\infty\phi_l^{0c})^2 + (\psi_l^{0c})^2\}^{-\frac{1}{2}}. \tag{4.10}$$

[It may be expedient to solve (4.5) and (4.8) by regarding them as initial conditions for the numerical integration of the Riccati equation (2.9) and then determining the zeros of $\chi(0, \beta)$. This procedure may be expedited by the Pruffer transformation $\chi = \tan\gamma$.]

5. Green's function for the half-space

We define the Green's function $G(x, y)$ for the half-space $x > 0$ as that dimensionless, line-source solution of (2.2) which satisfies

$$iG_x = \delta(y) \quad (x = 0) \tag{5.1}$$

together with finiteness and radiation conditions as x and/or $|y| \uparrow \infty$. Multiplying G by $I\sigma/gh_0$ yields a source with a peak volume flux of I into $x > 0$. The known result for constant depth is

$$G = \tfrac{1}{2}H_0^{(2)}(kR), \quad R = (x^2+y^2)^{\frac{1}{2}} \quad (h = \text{constant}). \tag{5.2a, b}$$

Posing the Fourier-transform pair

$$\mathscr{G}(x, \beta) = \int_{-\infty}^{\infty} G(x, y)\, e^{i\beta y}\, dy, \quad 2\pi G(x, y) = \int_{-\infty}^{\infty} \mathscr{G}(x, \beta)\, e^{-i\beta y}\, d\beta \tag{5.3a, b}$$

and transforming (2.2) and (5.1), we find that $\mathscr{G}(x, \beta)$ must satisfy (2.5) and

$$i\mathscr{G}_x = 1 \quad (x = 0). \tag{5.4}$$

The radiation and finiteness conditions imply that $\mathscr{G}$ must be proportional to $\exp(-\mu x)$ in $x > l$, where μ is given by (4.4) and is either positive-real for $\beta^2 > k_\infty^2$

or positive-imaginary (thereby satisfying the radiation condition as $x \uparrow \infty$) for $0 \leqslant \beta^2 < k_\infty^2$. Matching this solution to a linear combination of $\phi^{0c}(x)$ and $\phi^{0s}(x)$ in $(0, l)$, we obtain

$$(i/h_0)\,\mathscr{G}(x,\beta) = \begin{cases} \phi^{0s}(x) - (1/\chi_0)\,\phi^{0c}(x) & (0 \leqslant x \leqslant l), \quad (5.5a) \\ \{\phi_l^{0s} - (\phi_l^{0c}/\chi_0)\}\,e^{-\mu(x-l)} & (x \geqslant l), \quad (5.5b) \end{cases}$$

where

$$\chi_0 = (\psi_l^{0c} + \chi_\infty \phi_l^{0c})/(\psi_l^{0s} + \chi_\infty \phi_l^{0s}) \quad (5.6a)$$

is the inverse of (3.6b) and

$$\chi_\infty = \mu h_\infty = i\kappa_\infty. \quad (5.6b)$$

Invoking the fact (see §3) that $\phi^{0c}(x,\beta)$ and $\phi^{0s}(x,\beta)$ are entire functions of β, we find that the only finite singularities of $\mathscr{G}(x,\beta)$ in the complex-β plane are the branch points of χ_∞ at $\beta = \pm k_\infty$ and the poles of $1/\chi_0$ at $\beta = \pm \beta_m$, corresponding to the trapped modes defined by (4.3) and (4.5). Invoking the asymptotic representations

$$\phi^{0c} \sim (h_0/h)^{\frac{1}{2}} \cosh \beta x, \quad \phi^{0s} \sim \beta^{-1}(h_0 h)^{-\frac{1}{2}} \sinh \beta x \quad (\beta \to \infty), \quad (5.7a,b)$$

we find that $\mathscr{G}(x,\beta)$ is exponentially bounded as $\beta \to \infty$ if $x > 0$ and is $O(1/\beta)$ as $\beta \to \infty$ if $x = 0$.

We proceed on the assumption that k_∞ has a small, negative imaginary part, say $-ik_i$, and choose the branch cuts for μ along $\mathscr{R}\mu = 0$, such that $\mathscr{R}\mu > 0$ in the cut plane (the branch cuts, as sketched in figure 1, are those sections of the equilateral hyperbola through $\beta = \pm k_\infty$ that lie in $|\mathscr{R}\beta| < |\mathscr{R}k_\infty|$). The poles of $\mathscr{G}(x,\beta)$ then lie just below/above the real axis in $|\mathscr{R}k_\infty| < \pm\mathscr{R}\beta < |\mathscr{R}k_0|$. By deforming the path of integration for (5.3b) from the real axis into $\mathscr{I}\beta \lesseqgtr 0$ for $y \lesseqgtr 0$ and invoking Cauchy's residue theorem and the aforementioned bounding of $\mathscr{G}(x,\beta)$ as $\beta \to \infty$ on the assumption that x and/or $|y| > 0$, we obtain

$$G(x,y) = \sum_{m=1}^{n} \rho_m \phi(x,\beta_m)\,e^{-i\beta_m|y|} + G_C(x,y), \quad (5.8)$$

where

$$\rho_m = \operatorname{Res}\{h_0/\chi_0\}_{\beta=\beta_m} = [\{\phi_l^{0c}\,\partial_\beta(\psi_l^{0c} + \chi_\infty \phi_l^{0c})\}_{\beta=\beta_m}]^{-1} h_0 \quad (m \geqslant 1), \quad (5.9)$$

$$2\pi G_C(x,y) = \int_C \{ih_0/\chi_0(\beta)\}\,\phi(x,\beta)\,e^{-i\beta|y|}\,d\beta, \quad (5.10)$$

C traverses the branch cut from $\beta = k_\infty$ in a clockwise direction, and $\phi(x,\beta)$ is the analytical continuation of the right-hand side of (4.3) along C.

We restrict the further reduction of G to the neighbourhood $k_0|r| \ll 1$, which suffices for most applications (see §8 below) and permits both $\phi(x,\beta) = \phi^{0c}(x)$ and $\exp(-i\beta|y|)$ to be approximated by unity except for large β. Invoking these approximations in (5.8) and (5.10), remarking that $\chi_0(\beta)$ on the left-hand (or top) side of C is the complex conjugate of $\chi_0(\beta)$ on the right-hand (or bottom) side, letting $k_i \downarrow 0$, introducing the change of variable $\beta = -iv$ and the approximation [which follows from (5.7a) for $|\beta| \gg k_0$ and $k_0 x \ll 1$] $\phi(x,\beta) = \cos(vx)$ along $(-i\infty, 0)$, and substituting the resulting approximation to G_C into (5.8), we obtain

$$G(x,y) = \{\rho + i\lambda(x,y)\}\{1 + O(k_0 y)\}, \quad (5.11)$$

where

$$\rho = \sum_{m=0}^{n} \rho_m, \quad \pi\rho_0 = \int_0^{k_\infty} F(\beta)\,d\beta \quad (\mathscr{I}\beta \downarrow 0), \quad (5.12a,b)$$

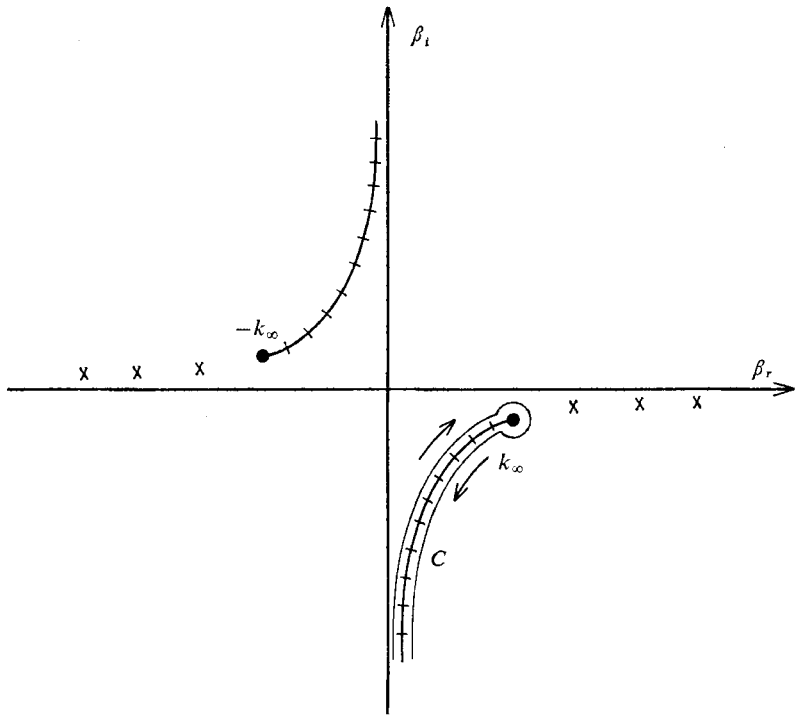

FIGURE 1. Location of poles (×) and branch cuts in complex-β plane (for two-step model of § 6) on the assumption that k_∞ has a small, negative imaginary part $-ik_i$. The cut from the branch point at $+k_\infty$ tends to the real-axis segment $(0, k_\infty)$ plus the negative imaginary axis $(-i\infty, 0)$ as $k_i \downarrow 0$; similarly, the cut from $-k_\infty$ tends to $(-k_\infty, 0)$ plus $(0, i\infty)$. C, the path of integration for $G_C(x, y)$, as given by (5.10), must be indented over/under the branch point (●) and poles (×) on the positive/negative real axis in the limit $k_i \downarrow 0$ and may be deformed into a contour around the lower/upper cut for $y \gtrless 0$ after allowing for the contributions of the poles. The sketch shows C for $y > 0$.

ρ_m is given by (5.9) for $m \geqslant 1$,

$$\pi\lambda(x, y) = \int_0^\infty F(-iv)\, e^{-v|y|} \cos(vx)\, dv, \tag{5.13}$$

and

$$F(\beta) = \mathscr{R}(ih_0/\chi_0) = (\alpha h)_\infty [\{(\alpha h)_\infty \phi_l^{0c}\}^2 + \{\psi_l^{0c}\}^2]^{-1} h_0. \tag{5.14}$$

The parameter ρ is a measure of the rate at which energy is radiated into $x > 0$ (see § 8 below). The distributions of the radiated energy among the trapped modes (which are radiated along the coast) and the continuous spectrum of the abyss are proportional to ρ_m $(m = 1, 2, \ldots, n)$ and ρ_0, respectively. The function λ is a measure of the non-radiated energy in the neighbourhood of the source (this non-radiated energy would be infinite for a concentrated source with a finite volume flux, but is finite for any integrable velocity distribution over a finite interval).

It follows from potential theory that iG, and hence $-\lambda$, is singular like $(1/\pi)\log R$ as $R \downarrow 0$. Referring to the limiting form of (5.2) as $kR \downarrow 0$, we surmise that

$$\pi\lambda(x, y) = -\ln(\tfrac{1}{2}\gamma k_0 R) + \mathscr{C} + O(k_0 R) \quad (k_0 R \downarrow 0), \tag{5.15}$$

where $\ln\gamma$ is Euler's constant and $\mathscr{C}$ is a constant – or, more precisely, a functional of h'/kh – that vanishes for $h =$ constant. We give derivations for specific examples

in the following sections and find that $\mathscr{C}$ is typically small if h does not vary rapidly over the coastal terminus of the shelf. Moreover, if $h(x)$ does vary rapidly over a terminal section that is small compared with $1/k_0$, we may replace that section by a discontinuity in h and invoke the continuity of χ across such a discontinuity (see last sentence in penultimate paragraph of §2) to obtain

$$G(x,y) = (h_0^-/h_0^+)\,(\rho + i\lambda)_+, \tag{5.16}$$

where $h_0^\pm$ are the depths at $x = 0_\pm$, and ρ and λ are based on h_0^+.

6. Two-step model

The simplest model of a continental shelf is a plateau of constant depth h_s in $0 < x < l$, terminating in vertical cliffs at $x = 0$ and $x = l$, such that

$$h(x) = \begin{cases} h_s & (0 < x < l), \quad (6.1a) \\ h_\infty & (x > l). \quad (6.1b) \end{cases}$$

We characterize this model by the dimensionless parameters

$$\hbar = (h_s/h_\infty) = (k_\infty/k_s)^2 \tag{6.2a}$$

and

$$\alpha_* l = (k_s^2 - k_\infty^2)^{\frac{1}{2}} l = k_s l(1-\hbar)^{\frac{1}{2}}, \tag{6.2b}$$

where α_* is defined as in (4.6).

The basic solutions on the shelf are

$$\phi^{0c}(x) = \cos\alpha x \quad \text{and} \quad \phi^{0s}(x) = (\alpha h_s)^{-1}\sin\alpha x \quad (0 < x < l), \tag{6.3a,b}$$

where

$$\alpha = (k_s^2 - \beta^2)^{\frac{1}{2}}. \tag{6.4}$$

Invoking (5.6), we obtain

$$\chi_l^{0c}(\beta) = \alpha h_s \tan\alpha l \tag{6.5a}$$

and

$$\chi_0(\beta) = \alpha h_s(\mu - \hbar\alpha\tan\alpha l)/(\hbar\alpha + \mu\tan\alpha l). \tag{6.5b}$$

Expressing β and μ as functions of α,

$$\beta = (k_s^2 - \alpha^2)^{\frac{1}{2}} \quad \text{and} \quad \mu = (\alpha_*^2 - \alpha^2)^{\frac{1}{2}}, \tag{6.6a,b}$$

we rewrite the trapped-mode equation (4.5) in the form (see figure 2)

$$(\alpha_*^2 - \alpha_m^2)^{\frac{1}{2}} = \hbar\alpha_m \tan\alpha_m l \quad (0 < \alpha_1 < \alpha_2 < \ldots \alpha_n < \alpha_*), \tag{6.7a}$$

where

$$n = 1 + [\alpha_* l/\pi] \tag{6.7b}$$

($[\alpha_* l/\pi] \equiv$ integral part of $\alpha_* l/\pi$). Similarly, we rewrite (4.8) and (4.10) in the forms

$$\tan\epsilon = \hbar\alpha(\alpha^2 - \alpha_*^2)^{-\frac{1}{2}}\tan\alpha l \quad (\alpha_* < \alpha < k_s) \tag{6.8}$$

and

$$A(\beta) = (\alpha^2 - \alpha_*^2)^{\frac{1}{2}}\{(\alpha^2 - \alpha_*^2)\cos^2\alpha l + \hbar^2\alpha^2\sin^2\alpha l\}^{-\frac{1}{2}} \tag{6.9a}$$

$$\uparrow A(0) = (\cos^2 k_s l + \hbar\sin^2 k_s l)^{-\frac{1}{2}} \quad (\beta^2 \downarrow 0). \tag{6.9b}$$

We note that $A(\beta) = 1$ for $\beta = k_\infty(1+\hbar)^{-\frac{1}{2}}$. $A(\beta)$ and ϵ are plotted in figures 3 and 4 for $\hbar = \frac{1}{6}$ (this value being appropriate for a two-step approximation to the shelf off California, e.g. $h_s = 600$ m and $h_\infty = 3600$ m). Increasing $k_s l$ by an integral multiple of π alters these results only slightly.

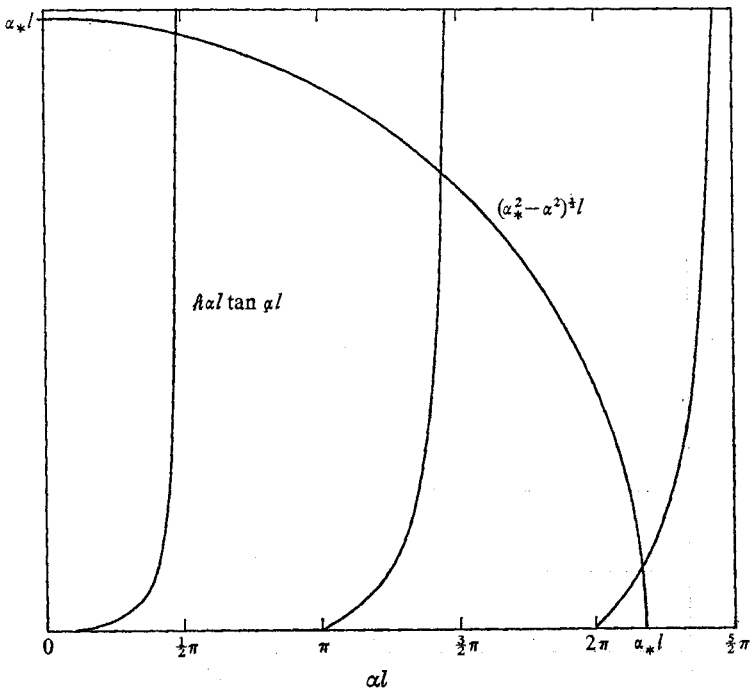

FIGURE 2. Graphical solution of (6.7) for $\hbar = \frac{1}{8}$ and $\alpha_s l = 2{\cdot}4\pi$ ($\alpha_* l = 2{\cdot}19\pi$).

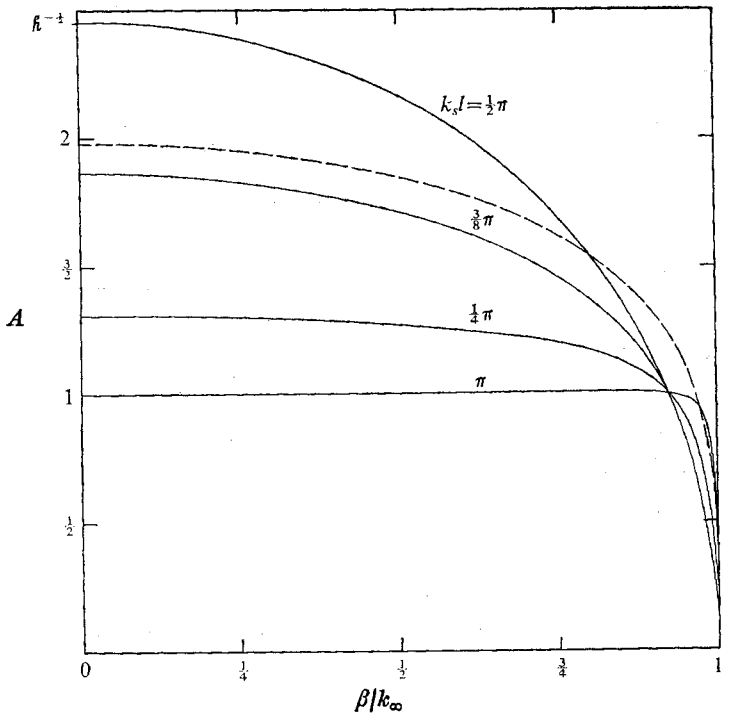

FIGURE 3. Amplification factor for the two-step model ($\hbar = \frac{1}{8}$), as given by (6.9). ————, WKB approximation (7.3*b*), with $h_s^{-\frac{1}{2}} = \frac{1}{2}(h_0^{-\frac{1}{2}} + h_\infty^{-\frac{1}{2}})$, such that k_s is the arithmetic mean of k_0 and k_∞ ($\hbar = \frac{1}{8}$ corresponds to $h_0/h_\infty = 0{\cdot}066$).

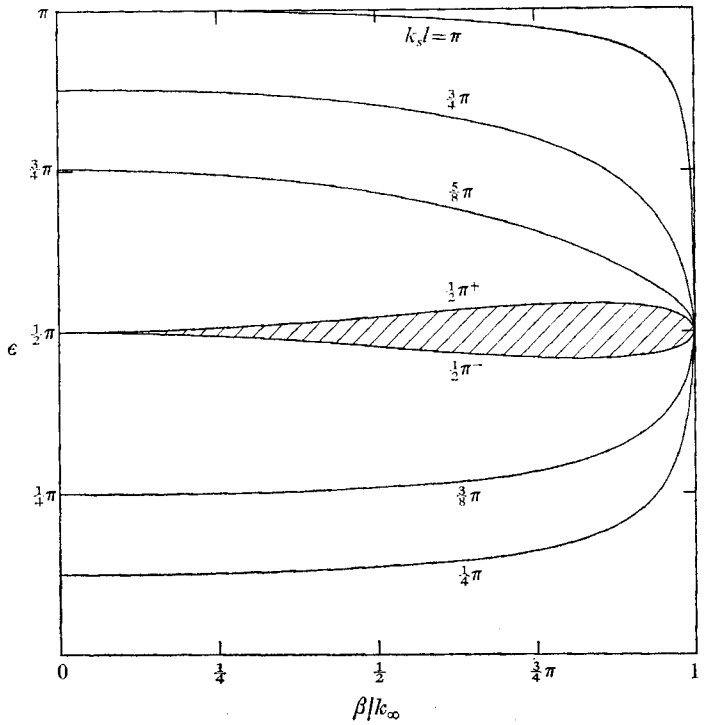

FIGURE 4. Phase parameter for the two-step model ($\hbar = \frac{1}{6}$), as given by (6.8) The shaded region is excluded by the discontinuity in ϵ at $k_s l = \frac{1}{2}\pi$.

Substituting (6.5*b*) into (5.9) and (5.12)–(5.14), we obtain

$$\rho_m = [(\beta_m l)\{1 + (\alpha_*/\mu)^2 (\alpha l)^{-1} \sin \alpha l \cos \alpha l\}_{\beta=\beta_m}]^{-1} \quad (m \geqslant 1), \tag{6.10}$$

$$\rho_0 = \frac{\hbar}{\pi}\int_0^{k_\infty} \frac{(k_\infty^2 - \beta^2)^{\frac{1}{2}}\, d\beta}{(k_\infty^2 - \beta^2)\cos^2 \alpha l + \hbar^2 \alpha^2 \sin^2 \alpha l}, \tag{6.11}$$

$$\lambda(x, y) = \frac{\hbar}{\pi}\int_0^{\infty} \frac{(k_\infty^2 + v^2)^{\frac{1}{2}}\, e^{-v|y|} \cos(vx)\, dv}{(k_\infty^2 + v^2)\cos^2\{l(k_s^2 + v^2)^{\frac{1}{2}}\} + \hbar^2 (k_s^2 + v^2)\sin^2\{l(k_s^2 + v^2)^{\frac{1}{2}}\}}. \tag{6.12}$$

The β_m and ρ_m may be approximated in various ways; however, their numerical evaluation is straightforward. Numerical values of ρ_m and $\sum_m \rho_m$ for $\hbar = \frac{1}{6}$ are plotted in figures 5(*a*) and (*b*). The plots for other $\hbar < 1$ are similar. The total ρ for $\hbar = 0{\cdot}1$, $0{\cdot}2$ and $0{\cdot}4$ is plotted in figure 6. The limiting value of ρ as either $\hbar \uparrow 1$ or $k_s l \downarrow 0$ is $\frac{1}{2}$.

The approximations

$$\alpha_m \uparrow (m - \tfrac{1}{2})\pi/l, \quad \rho_m \uparrow l^{-1}(k_s^2 - \alpha_m^2)^{-\frac{1}{2}} \quad (\hbar \downarrow 0) \tag{6.13}$$

are adequate for $m < n$, but not typically for $m = n$. They also are asymptotically valid for $k_* l \to \infty$ and yield

$$\sum_{m=1}^{n} \rho_m \sim \frac{1}{\pi}\int_0^{k_*} (k_s^2 - \alpha^2)^{-\frac{1}{2}}\, d\alpha = \frac{1}{\pi}\sin^{-1}(1 - \hbar)^{\frac{1}{2}} \quad (\alpha_* l \to \infty). \tag{6.14}$$

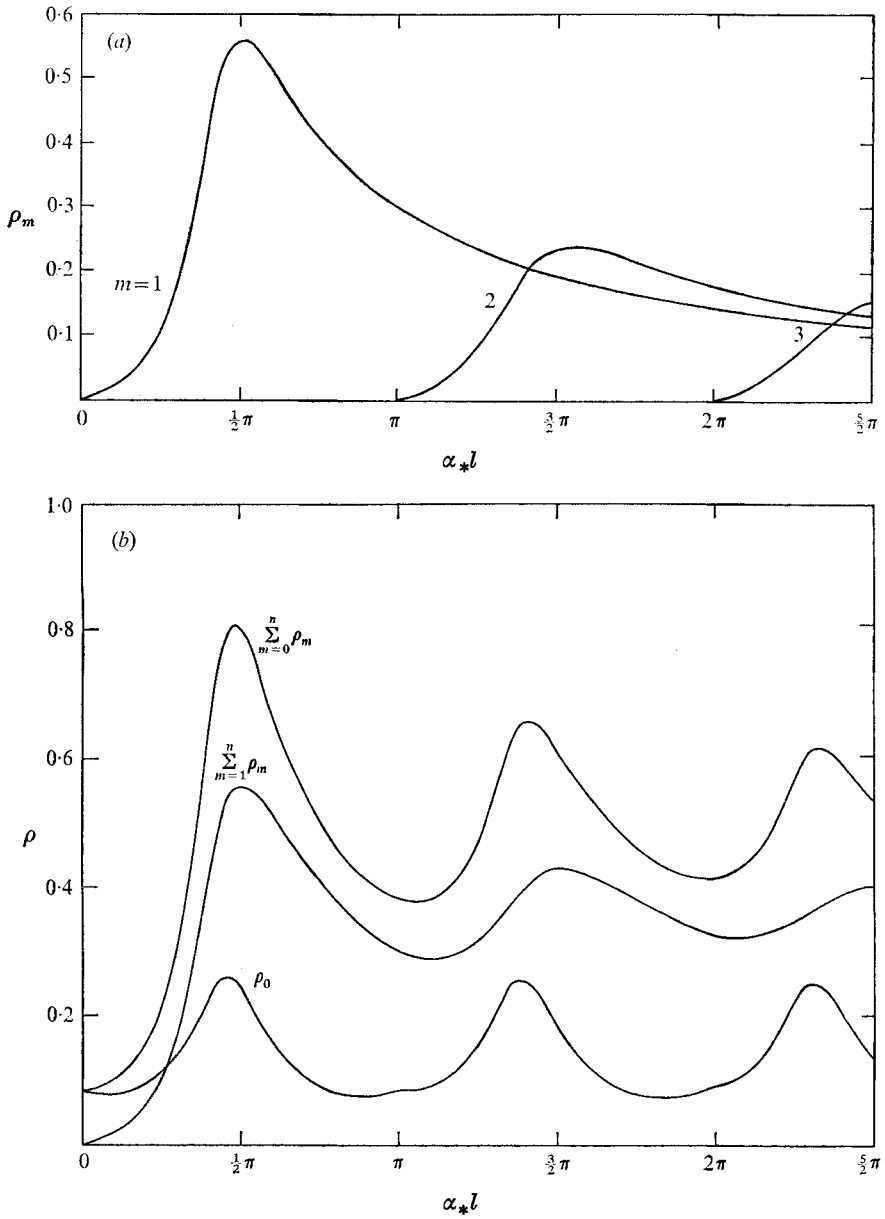

FIGURE 5. (*a*) The trapped-mode contributions to the dimensionless radiation resistance for the two-step model ($\hbar = \frac{1}{6}$). (*b*) The relative contributions of the trapped modes ($1 \leqslant m \leqslant n$) and the radiated modes ($m = 0$) to the radiation resistance for the two-step model ($\hbar = \frac{1}{6}$).

The corresponding approximation to ρ_0, as obtained by averaging the rapidly oscillating integrand in (6.11) over $\frac{1}{2}\pi$ intervals of αl, is

$$\rho_0 \sim \frac{1}{\pi}\int_0^{k_\infty} (k_3^2 - \beta^2)^{-\frac{1}{2}}\, d\beta = \frac{1}{\pi}\sin^{-1}\hbar^{\frac{1}{2}} \quad (\alpha_* l \to \infty). \tag{6.15}$$

Adding (6.14) and (6.15), we obtain the asymptotic limit $\rho \sim \frac{1}{2}$. This limit, which is analogous to that of geometrical optics for the scattering cross-section of an

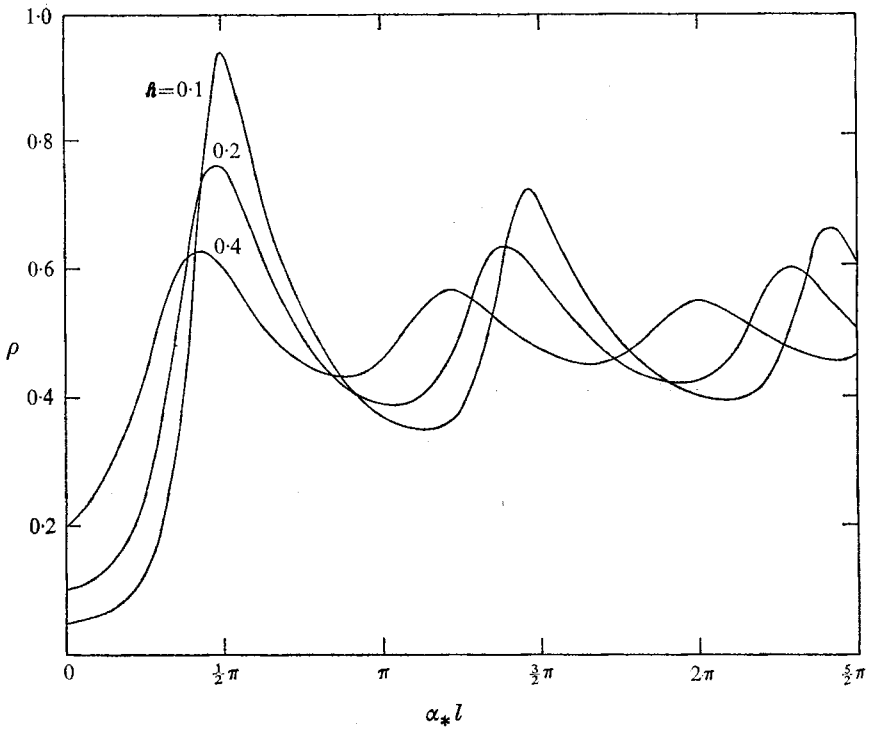

FIGURE 6. The dimensionless radiation resistance for the two-step model. The limiting result for an ocean of constant depth is $\rho = \frac{1}{2}$.

obstacle, is approached in an oscillatory manner (see figure 6), with the amplitude of the oscillations increasing with decreasing $\hat{h}$; however, it provides a rough approximation ($\pm 20\,\%$) for $\alpha_* l > \pi$ and $\hat{h} \geqslant 0{\cdot}2$.

It remains to evaluate λ. Introducing the change of variable $t = v|y|$ in (6.12) and averaging the rapidly oscillating integrand over $\frac{1}{2}\pi$ intervals of $(l/|y|)\,(k_s^2 y^2 + t^2)^{\frac{1}{2}}$ in the limit $|y|/l \to 0$, we obtain

$$\pi\lambda \sim \int_0^\infty (k_s^2 y^2 + t^2)^{-\frac{1}{2}} e^{-t} \cos(tx/y)\, dt \quad (|y|/l \to 0) \tag{6.16a}$$

$$= \mathscr{R} \int_0^\infty e^{-z \sinh \eta}\, d\eta \quad (z = k_s\{|y| + ix\}) \tag{6.16b}$$

$$= -\tfrac{1}{2}\pi \mathscr{R}\{\mathbf{E}_0(z) + Y_0(z)\} \tag{6.16c}$$

$$= -\ln(\tfrac{1}{2}\gamma k_s r) + O(k_s r) \quad (k_s r \downarrow 0), \tag{6.16d}$$

where (6.16c) follows from (6.16b) through the integral representation of the Anger–Weber function $\mathbf{E}_0$ (Watson 1945, §10·1 and §10·13), Y_0 is a Bessel function, and $\ln\gamma$ is Euler's constant. The approximation (6.16d) is equivalent to (5.15) with $h_0 = h_s$ and $\mathscr{C} = 0$.

7. Gradually sloping shelf

We now consider a gradually sloping shelf, $0 < x < l$, over which $h(x)$ increases monotonically from h_0 to h_∞, such that $\alpha^2(x,\beta) > 0$ if $\beta^2 < k_\infty^2$ and that $\alpha^2(x,\beta)$ has one and only one zero, say x_c, if $k_\infty^2 < \beta^2 < k_0^2$. We assume

$$s = s(x) \equiv \frac{1}{2}\frac{d\ln h}{dx} = \frac{d\ln(1/k)}{dx} \ll |\alpha| \tag{7.1}$$

at all points bounded away from $x = x_c$. Typical values of s for the Pacific coast are smaller than $0{\cdot}1\,\mathrm{km}^{-1}$ (e.g. $s = 0{\cdot}05\,\mathrm{km}^{-1}$ for a smoothed fit to the shelf in the first 70 km off Crescent City, over which h increases from 100 m to 3000 m); accordingly, $s \ll |\alpha|$ is likely to be satisfied over most of a typical continental shelf at tsunami wavelengths, although it may be violated at either the coastal or the abyssal terminus or both.

The asymptotic (Liouville) approximations

$$\phi^{0c}(x) \sim (\kappa_0/\kappa)^{\frac{1}{2}}\cos\left(\int_0^x \alpha\,dx\right), \quad \phi^{0s}(x) \sim (\kappa_0\kappa)^{-\frac{1}{2}}\sin\left(\int_0^x \alpha\,dx\right) \tag{7.2a,b}$$

hold for $-\infty < \beta^2 < k_\infty^2$ and, on substitution into (4.8) and (4.10), yield

$$\epsilon = \int_0^l \alpha\,dx \quad \text{and} \quad A = \left(\frac{h_\infty}{h_0}\right)^{\frac{1}{2}}\left(\frac{k_\infty^2-\beta^2}{k_0^2-\beta^2}\right)^{\frac{1}{4}}. \tag{7.3a,b}$$

The result (7.3*b*) is plotted in figure 3 for $h_0/h_s = 0{\cdot}066$, which corresponds to $\hbar = \frac{1}{6}$ for the two-step model, equation (6.9), if h_s is defined such that k_s is the arithmetic mean of k_0 and k_∞.

The WKB approximation (Jeffreys & Jeffreys 1950, §17.131)

$$\phi(x) \sim \begin{cases} \kappa^{-\frac{1}{2}}\sin\left(\int_x^{x_c}\alpha\,dx + \frac{1}{4}\pi\right) & (x < x_c) \qquad (7.4a) \\ \frac{1}{2}|\kappa|^{-\frac{1}{2}}\exp\left(-\int_{x_c}^x |\alpha|dx\right) & (x > x_c) \qquad (7.4b) \end{cases}$$

satisfies the finiteness condition (4.1*b*) and is valid for $\beta^2 > k_\infty^2$. By requiring it to satisfy (4.1*a*), we obtain the trapped-mode eigenvalue equation

$$\theta_c(\beta) \equiv \int_0^{x_c}\alpha\,dx = \int_\beta^{k_0}(k^2-\beta^2)^{\frac{1}{2}}(ks)^{-1}dk = (m-\tfrac{3}{4})\pi \quad (\beta = \pm\beta_m), \tag{7.5a}$$

where

$$m = 1, 2, \ldots, n, \quad n = [\tfrac{3}{4} + \pi^{-1}\theta_c(k_\infty)]. \tag{7.5b}$$

The input impedance implied by (7.2) and (7.5) is

$$\chi_0(\beta) \sim \begin{cases} i\kappa_0 & (\beta^2 < k_\infty^2), \qquad (7.6a) \\ \kappa_0\cot(\theta_c + \frac{1}{4}\pi) & (k_\infty^2 < \beta^2 < k_0^2), \qquad (7.6b) \\ |\kappa_0| & (\beta^2 > k_0^2). \qquad (7.6c) \end{cases}$$

[The apparent branch points at $\beta = \pm k_0$, rather than $\pm k_\infty$, are artifacts of the asymptotic approximation and do not affect the deformation of the Green's-function contour depicted in figure 1, which is antecedent to the asymptotic

approximation.] Substituting (7.6a) into (5.12)–(5.14) and (7.6b) into (5.9), we obtain (cf. equation (6.15))

$$\pi\rho_0 = \sin^{-1}(k_\infty/k_0) = \sin^{-1}(h_0/h_\infty)^{\frac{1}{2}}, \tag{7.7}$$

$$\rho_m = (k_0^2-\beta_m^2)^{-\frac{1}{2}}\{-\theta_c'(\beta_m)\}^{-1}, \tag{7.8}$$

and (5.15) with $\mathscr{C} = 0$. The asymptotic spacing of the β_m is, from (7.5), $\pi/\theta_c'(\beta_m)$; combining this result with (7.8), we obtain (cf. equation (6.14))

$$\pi\sum_{m=1}^{n}\rho_m \sim \int_{k_0}^{k_\infty}\rho_m\theta'(\beta_m)\,d\beta = \tfrac{1}{2}\pi-\sin^{-1}(k_\infty/k_0) \quad (k_0 l\to\infty), \tag{7.9}$$

which, in conjunction with (7.7), implies the asymptotic limit $\rho \sim \frac{1}{2}$, as in §6.

We obtain a first approximation to $\mathscr{C}$ by improving the approximation to $F(\beta)$. Rewriting (2.9) in the form

$$1/\chi = (i\kappa)^{-1}\{1+h(1/\chi)_x\}^{\frac{1}{2}} \quad (\mathscr{R}\chi > 0) \tag{7.10}$$

and proceeding by iteration from the first approximation

$$\chi(x,\beta) \sim i\kappa \quad (\beta^2 < k_\infty^2), \tag{7.11}$$

we obtain

$$F(\beta) \sim \alpha_0^{-1}[1-(s/\alpha)^2\{\tfrac{1}{2}-\tfrac{3}{2}(k/\alpha)^2+\tfrac{7}{8}(k/\alpha)^4 + (s'/\alpha^2)\{\tfrac{1}{2}-\tfrac{1}{4}(k/\alpha)^2\}+O(s/\alpha^4)\}]_{x=0} \quad (\beta^2 < k_\infty^2), \tag{7.12}$$

where $s(x)$ is given by (7.1), and

$$s' = ds/dx = ds^2/d\ln h. \tag{7.13}$$

Substituting (7.12) into (5.13), we find that the leading term may be evaluated as in (6.13), with h_s replaced by h_0, whilst the remaining terms may be evaluated from

$$\int_0^\infty \frac{e^{-vy}\,dv}{(k^2+v^2)^{n+\frac{1}{2}}} \sim \frac{(n-1)!\,2^{n-1}}{1.3.5\ldots(2n-1)\,k^{2n}}\{1+O(ky)\} \quad (n \geqslant 1). \tag{7.14}$$

The end result is (5.15) with

$$\mathscr{C} = [\tfrac{1}{30}(s/k)^2+\tfrac{1}{3}(s'/k^2)+O\{(s/k)^4\}]_{x=0_+}. \tag{7.15}$$

The asymptotic approximation (7.12) is not uniformly valid in the neighbourhood of $\beta = k_\infty$ and therefore is not generally suitable for the calculation of ρ_0. However, $h_0 \ll h_\infty$ in actual applications, and we may obtain an approximation to ρ_0 that is consistent with (5.15), but with an additional error factor of $1+O(h_0/h_\infty)$, simply by approximating α by k_0 in (7.12), the substitution of which into (5.12b) then yields

$$\rho_0 = (k_\infty/\pi)\,F(0)\{1+O(h_0/h_\infty)\} \tag{7.16a}$$

$$\sim \pi^{-1}(h_0/h_\infty)^{\frac{1}{2}}\{1+\tfrac{1}{8}(s/k)^2+\tfrac{1}{4}(s'/k^2)\}_{x=0_+}. \tag{7.16b}$$

Parabolic shelf

We apply the preceding results to a parabolic profile of latus rectum b with vertex at $x = -d$ and $h = 0$ (such that $bh_0 = d^2$):

$$h(x) = (x+d)^2/b \quad (0 < x < l). \tag{7.17}$$

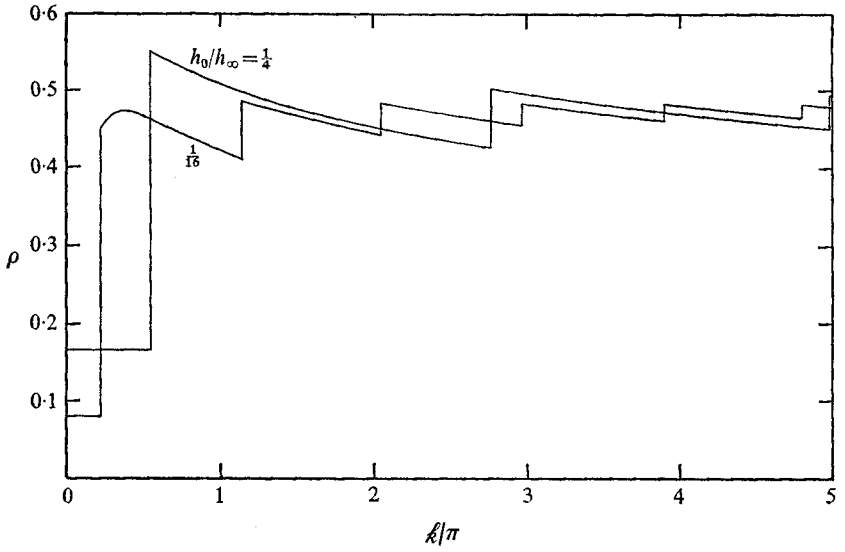

FIGURE 7. The dimensionless radiation resistance for the gradually sloping, parabolic shelf, as calculated from the WKB approximation in §7.

Invoking (2.3) and (7.1), we obtain

$$k/\kappa = s = (x+d)^{-1}, \quad \kappa = \sigma(b/g)^{\frac{1}{2}}. \tag{7.18a,b}$$

Substituting (7.17) and (7.18) into (7.5) and (7.8), we obtain the asymptotic solution (as $\kappa \uparrow \infty$) for the trapped-mode parameters in the parametric form

$$\beta_m = k_0 \operatorname{sech} v_m, \tag{7.19a}$$

$$\theta_{0c}(\beta_m) = \kappa(v_m - \tanh v_m) = (m - \tfrac{3}{4})\pi, \tag{7.19b}$$

$$\rho_m = \kappa^{-1} \operatorname{cosech} v_m \coth v_m, \tag{7.19c}$$

and

$$n = [\tfrac{3}{4} + (\kappa/\pi)(v_\infty - \tanh v_\infty)], \tag{7.19d}$$

where

$$v_\infty = \cosh^{-1}(k_0/k_\infty) = \cosh^{-1}\{1 + (l/d)\} \tag{7.20a}$$

and

$$h_0/h_\infty = \operatorname{sech}^2 v_\infty. \tag{7.20b}$$

Substituting (7.18) into (7.15), we obtain

$$\mathscr{C} = -\tfrac{3}{10}\kappa^{-2} + O(\kappa^{-4}). \tag{7.21}$$

The radiation resistance obtained by substituting (7.7) and (7.19*c*) into (5.12*a*) is plotted in figure 7 for $h_0/h_\infty = \frac{1}{4}$ and $\frac{1}{16}$. The discontinuities in ρ, which represent the entry of additional trapped modes, are a consequence of the non-uniform validity of the WKB approximation in the neighbourhood of $\beta = k_\infty$; cf. figure 6, where ρ changes sharply but continuously. [The parabolic profile permits an exact solution of (2.5) in terms of modified Bessel functions of order $(\frac{1}{4} - \kappa^2)^{\frac{1}{2}}$. Limited calculations with this solution yielded numerical results for ρ that are qualitatively similar to those of figure 6.]

An extension of the results of this section to a gradually sloping shelf that terminates at a vertical drop from h_l to h_∞ at $x = l$ reveals that the primary effect of such a discontinuity is to increase, and render oscillatory with k_0, the contribution of the continuous spectrum to the radiation resistance (cf. ρ_0 in figure 5(*b*)),

although it also has lesser effects on the trapped modes. The net effect on ρ is, in any event, small for sufficiently large values of $k_0 l$, say $k_0 l \gtrsim 2\pi$, if $h_0/h_\infty \ll 1$. The effect on λ also is small, both because λ is dominated by the logarithmic term in (5.15) and because it is derived from integration over the entire imaginary axis of the β plane, over most of which the effects of slope are small, and it appears that (7.15) provides an adequate estimate of $\mathscr{C}$ for an appropriately smoothed profile. The effects of a locally steep slope at the coastal terminus of the shelf, over an x interval that is small compared with $1/k$, may be incorporated simply by choosing h_0 as the depth at the seaward end of this interval (see last paragraph in §5).

8. Resonant response of harbours

Following an earlier analysis (Miles 1971, hereinafter designated by I) for a constant-depth model, we consider the effect of a continental shelf on the resonant response of a harbour to an incoming tsunami. This response is essentially restricted to the Helmholtz mode if, as is almost always true, the dimensions of both the harbour and its entry channel are small compared with the *local* wavelength ($1/k$ based on the harbour depth) of the tsunami. Our notation and conventions follow I except as follows: the signs of x and u are reversed; j and ω in I appear here as i and σ; G denotes the Green's function for the harbour in I, wherein the Green's function for the half-space is given by the right-hand side of (5.2) above.

Let $\zeta_0 + \zeta_s$ be the total disturbance in $x > 0$, where ζ_0 is the disturbance that would exist if there were no flow across $x = 0$ ($\partial\zeta_0/\partial x = 0$ at $x = 0$), and ζ_s is the scattered wave that is induced by the flow through the harbour mouth, M, in $x = 0$. It follows from (2.2a) and the definition of the Green's function in §5 that

$$\zeta_s(x, y) = (\sigma/g)\int_M G(x, y-\eta)\, u(0, \eta)\, d\eta, \tag{8.1}$$

where u is the x component of $\mathbf{u}$. The total flow into M is

$$\int_M uh\, dy \equiv I, \tag{8.2}$$

where I is the current flowing into the equivalent circuit of I in response to the input voltage (see I, §3 for details)

$$V_i = (\zeta_0)_M. \tag{8.3}$$

The corresponding radiation impedance, which must be placed in series with the harbour impedance (including that of its entry channel, if any) to obtain the complete equivalent circuit, is

$$Z_M = R_M + iX_M = |I|^{-2}\int_M \zeta_s u^* h\, dy, \tag{8.4}$$

where u^* is the complex conjugate of u. Substituting (8.1) into (8.4) and introducing the normalized velocity distribution $f(y)$, such that

$$(uh)_M = If(y), \quad \int_M f(y)\, dy = 1, \tag{8.5a, b}$$

we obtain (cf. I, equation (3.4))

$$Z_M = (\sigma/gh_0^-)\int_M\int_M G(0, y-\eta)f(\eta)f^*(y)\,d\eta\,dy, \tag{8.6}$$

where h_0^- is the inner coastal depth ($x = 0_-$) and may differ from h_0^+, the outer coastal depth, in consequence of the approximation of the terminal section of the continental shelf by a discontinuity in depth.

The complete formulation of the scattering problem requires the construction of an integral equation for $f(y)$ through the matching of the exterior solution provided by (8.1) to an appropriate solution in the harbour ($x < 0$). It suffices for our purposes, however, to construct (as in I) a variational approximation to Z_M by invoking the potential-flow approximation†

$$f(y) = (1/\pi)\{(\tfrac{1}{2}a)^2 - y^2\}^{-\frac{1}{2}} \quad (|y| < \tfrac{1}{2}a), \tag{8.7}$$

where a, the width of M, is, by hypothesis, small compared with $1/k_0$, and the normalization corresponds to (8.5b). Substituting (5.16) and (8.7) into (8.6), we obtain

$$Z_M = (\sigma/gh_0^+)\,[\rho + (i/\pi)\{-\ln(\tfrac{1}{8}\gamma k_0^+ a) + \mathscr{C}\}], \tag{8.8}$$

where k_0^+ is the wavenumber based on h_0^+. The corresponding result for a constant-depth ocean, as given by equations (3.7) and (3.9) of I, is

$$Z_M = (\sigma/gh)\,[\tfrac{1}{2} - (i/\pi)\ln(\tfrac{1}{8}\gamma ka)], \tag{8.9}$$

where k is based on h.

The appearance of h_0^+ in (8.8) *vis-à-vis* h in (8.9) follows directly from conservation of mass flux and free-surface displacement across M and does not depend on the variation of $h(x)$ over the shelf; in particular, setting $\rho = \frac{1}{2}$ and $\mathscr{C} = 0$ in (8.8) extends the model of I to an ocean of constant depth h_0^+ that may differ from the depth of the harbour. The appearances of ρ in place of $\frac{1}{2}$ and of $\ln k_0^+ - \mathscr{C}$ in place of $\ln k$ reflects the change in depth, from h_0^+ to h_∞, over the shelf. The principal effects of these differences are to raise the resonant frequency, the inverse damping factor Q, and the power-spectrum amplification factor $\mathscr{P}$ (ratio of the mean-square elevation in the harbour to the mean-square elevation that would exist at the coastline if the tsunami were specularly reflected). The increase in the resonant frequency is not likely to exceed 50 % for a harbour without an entry channel and is likely to be small for a harbour with a significant entry channel. The predicted increases in Q and $\mathscr{P}$ may be large; however, dissipation, which reduces both Q and $\mathscr{P}$, would then be relatively more important. The variation of ρ with k might be significant (within the accuracy justified by the basic model) if the shelf were so short that the first trapped mode were below resonance for the tsunami (so that ρ is on the steeply rising portion of the first peak in the radiation-resistance curve, see figures 5(b) and 7); otherwise the rough approximation $\rho = \frac{1}{2}$ is likely to be adequate.

This work was partially supported by the National Science Foundation, under Grant NSF-GA-10324, and by the Office of Naval Research, under Contract N00014-69-A-0200-6005.

† The results in I imply that R_M is independent of, and X_M is quite insensitive to, the form of $f(y)$ for $k_0 a \ll 1$.

REFERENCES

INCE, E. L. 1944 *Ordinary Differential Equations*. Dover.

JEFFREYS, H. & JEFFREYS, B. S. 1950 *Methods of Mathematical Physics*. Cambridge University Press.

LAMB, H. 1932 *Hydrodynamics*. Cambridge University Press.

MILES, J. W. 1971 Resonant response of harbours: an equivalent-circuit analysis. *J. Fluid Mech.* **46**, 241–265.

MUNK, W., SNODGRASS, F. & GILBERT, F. 1964 Long waves on the continental shelf: an experiment to separate trapped and leaky modes. *J. Fluid Mech.* **20**, 529–554.

WATSON, G. N. 1945 *A Treatise on the Theory of Bessel Functions*. Cambridge University Press.